Structural Effects of Covalent Inhibition of Phospholipase A_2 Suggest Allosteric Coupling between Membrane Binding and Catalytic Sites

Suren A. Tatulian
Biomolecular Science Center and Department of Molecular Biology and Microbiology, University of Central Florida, Orlando, Florida 32826

ABSTRACT Phospholipase A_2 (PLA_2) binds to membranes and catalyzes phospholipid hydrolysis, thus initiating the biosynthesis of lipid-derived mediators of inflammation. A snake-venom PLA_2 was completely inhibited by covalent modification of the catalytic histidine 48 by *p*-bromophenacyl bromide. Moreover, His^{48} modification affected PLA_2 structure, its membrane-binding affinity, and the effects of PLA_2 on the membrane structure. The native PLA_2 increased the order parameter of fluid membranes, whereas the opposite effect was observed for gel-state membranes. The data suggest membrane dehydration by PLA_2 and the formation of PLA_2-membrane hydrogen bonding. The inhibited PLA_2 had lower membrane-binding affinity and exerted weaker effects on membrane hydration and on the lipid-order parameter. Although membrane binding resulted in formation of more flexible α-helices in the native PLA_2, which corresponds to faster amide hydrogen exchange, the modified enzyme was more resistant to hydrogen exchange and experienced little structural change upon membrane binding. The data suggest that 1), modification of a catalytic residue of PLA_2 induces conformational changes that propagate to the membrane-binding surface through an allosteric mechanism; 2), the native PLA_2 acquires more dynamic properties during interfacial activation via membrane binding; and 3), the global conformation of the inhibited PLA_2, including the α-helices, is less stable and is not influenced by membrane binding. These findings provide further evidence for an allosteric coupling between the membrane-binding (regulatory) site and the catalytic center of PLA_2, which contributes to the interfacial activation of the enzyme.

INTRODUCTION

Secretory phospholipases A_2 (PLA_2) are relatively small (13–15 kDa) water-soluble enzymes that are able to bind to cellular membranes and hydrolyze the *sn*-2 ester bond of glycerophospholipids (Six and Dennis, 2000; Berg et al., 2001). Degradation of phospholipids by PLA_2 produces lysophospholipids and free fatty acids including arachidonic acid, which may be metabolized, respectively, to platelet-activating factor and eicosanoids, which are potent mediators of inflammation, allergy, apoptosis, and cancer (Valentin et al., 1999; Bezzine et al., 2000; Touqui and Alaoui-El-Azher, 2001). Elucidation of the catalytic and regulatory mechanisms of these enzymes is important both for developing more efficient antiinflammatory therapies and for understanding the fundamental principles of interfacial enzymology.

Biochemical and crystallographic studies led to a catalytic mechanism that involves a His^{48}-Asp^{99} doublet, a conserved water molecule that donates a proton to His^{48} and performs nucleophilic attack on the *sn*-2 ester bond of the substrate, and a Ca^{2+} cofactor ion (Verheij et al., 1980; Scott et al., 1990). The collapse of the tetrahedral intermediate is followed by deprotonation of His^{48} by the *sn*-2 oxygen of the lysophospholipid. More recent experimental evidence has suggested an alternative mechanism that involves two water molecules. One is the nucleophilic water that is in the inner coordination sphere of Ca^{2+}, and the other is an assisting water that is in the outer coordination sphere of Ca^{2+} and is H-bonded to His^{48} (Yu et al., 1998; Epstein et al., 2001). Despite distinct differences between these two mechanisms, in both cases, the central events in the catalytic reaction are the protonation and deprotonation of the imidazole ring of His^{48}.

Divergent regulatory mechanisms of secretory PLA_2s are currently under consideration. The major fact is that the binding of PLA_2 to the surface of aggregated substrate such as membranes or micelles substantially increases the enzyme activity, an effect known as interfacial activation (Pieterson et al., 1974; Verger and de Haas, 1976; Jain and Berg, 1989; Gelb et al., 1995, 1999; Yu et al., 2000). Similar crystal structures of PLA_2 without and with bound inhibitors, plus the unequivocal fact that PLA_2 activity can be modulated by the physical properties of the aggregated phospholipid, led to a hypothesis that substrate-related factors such as increased local concentration or productive positioning of the substrate rather than structural changes in the enzyme account for the interfacial activation of PLA_2 (Scott et al., 1990; Scott and Sigler, 1994a; Burack and Biltonen, 1994; Burack et al., 1997). Although the regulatory effect of the interface is unarguable, the key and still-unanswered question is whether PLA_2 undergoes functionally important structural changes during interfacial activation.

Currently there is increasing evidence that allosteric effects are probably involved in PLA_2 activation. Modification of PLA_2 residues that directly interact with membranes but do not participate in catalysis have been shown to modulate both interfacial binding and the catalytic activity of the enzyme (Liu et al., 1995; Han et al., 1997; Baker et al., 1998; Yu et al., 1999, 2000). On the other hand, His^{48} mutations caused structural perturbations involving the

Submitted May 23, 2002, and accepted for publication October 24, 2002.
Address reprint requests to Dr. Suren A. Tatulian, Biomolecular Science Center and Dept. of Molecular Biology and Microbiology, University of Central Florida, 12722 Research Parkway, Orlando, FL 32826. Tel.: 407-207-4996; Fax: 407-384-2816; E-mail: statulia@mail.ucf.edu.

0006-3495/03/03/1773/11 $2.00

N-terminal α-helix of PLA_2, which plays important roles in both membrane binding of the enzyme and substrate binding to the catalytic center (Li and Tsai, 1993; Yuan et al., 1999; Sekar et al., 1999). These findings suggest a possible allosteric coupling between the membrane-binding surface (the regulatory site) and the catalytic residues of PLA_2. In accord with these findings, our previous studies indicated that membrane-surface properties not only affect the membrane-binding strength of PLA_2, but also modulate the dynamic structure of the enzyme that correlates with its catalytic activity (Tatulian, 2001). These results led to a reciprocal mechanism of interfacial activation of PLA_2, which implies that both membrane-surface properties and conformational changes in PLA_2 are mutually related, synergistic determinants of PLA_2 activation. The aim of the present work was to provide more insight into the regulatory mechanism of PLA_2 by providing further evidence for the allosteric coupling between membrane binding and catalytic sites of PLA_2. The catalytic His^{48} residue of PLA_2 has been covalently modified by *p*-bromophenacyl bromide (pBPB), which is known to completely inhibit PLA_2 activity by binding to the imidazole group of His^{48} and abolishing its general base function (Volwerk et al., 1974; Yang and King, 1980; Renetseder et al., 1988; Zhao et al., 1998). The results of the experiments on PLA_2 free in solution and bound to phospholipid membranes as well as under catalytic and noncatalytic conditions (i.e., in the presence and absence of Ca^{2+}) indicate significant effects of His^{48} modification on the membrane-binding properties of PLA_2, the influence of PLA_2 on the membrane structure, and membrane-induced structural changes in the enzyme. Together, the data suggest that covalent modification of a catalytic residue of PLA_2 affects the enzyme conformation and these conformational effects propagate to the membrane-binding surface, which probably involves an allosteric mechanism that couples the active site of PLA_2 to its membrane-binding surface.

MATERIALS AND METHODS

Materials

PLA_2 was purified from the venom of the snake *Agkistrodon piscivorus piscivorus* (Sigma, St. Louis, MO), as previously described (Maraganore et al., 1984; Cho and Shen, 1999). PLA_2 was covalently modified by incubation with a 10-fold molar excess of pBPB in a buffer that contained 100 mM sodium cacodylate/HCl (pH 6.0) and 100 mM NaCl at 30°C, as described (Volwerk et al., 1974). The purity of the product was confirmed by complete loss of lipolytic activity. The lipids were purchased from Avanti Polar Lipids (Alabaster, AL), pBPB was from Fluka (Milwaukee, WI), and the other chemicals were from Sigma.

FTIR, fluorescence, and circular dichroism experiments

Attenuated total reflection-Fourier transform infrared (ATR-FTIR) experiments were carried out as described (Tatulian, 2001). Briefly, a phosphatidylcholine monolayer was first deposited on a germanium internal-reflection plate (Spectral Systems, Irvington, NY) by the Langmuir-Blodgett technique. The plate with the monolayer was assembled in an ATR sample cell, followed by the injection of vesicles of desired lipid composition into the cell and spontaneous formation of supported lipid bilayers. PLA_2 was injected into the ATR cell and allowed to adsorb to the supported membranes for ~5 min. ATR-FTIR spectra were recorded using a Nicolet 740 or a Vector 22 infrared spectrometer (Nicolet Analytical Instruments, Madison, WI and Bruker Optics, Billerica, MA) at a spectral resolution of 2 cm^{-1}. The ATR dichroic ratios (R^{ATR}) were determined by dividing the absorbance intensities of a given band measured at parallel ($A_\parallel$) and perpendicular ($A_\perp$) polarizations of the light: $R^{ATR} = A_\parallel/A_\perp$.

The amide hydrogen-exchange (HX) experiments were done as described (Tatulian et al., 1998a). After recording several spectra in the H_2O buffer, the ATR sample cell was flushed with 10 volumes of a D_2O buffer. The time point of the first exposure of the membrane-bound protein to D_2O was taken as the zero time of HX. The number of scans per spectrum was gradually increased from 128 to 1024, and the time interval between successive spectra was correspondingly increased from 1 to 30 min, taking into account the exponential nature of HX kinetics.

Nonradiative energy transfer (NET) from the tryptophans of PLA_2 to dansyl-phosphatidylethanolamine (DPE, 10 mol % in sonicated vesicles) was measured using a SPEX Fluoromax spectrofluorometer (Instruments S. A., Edison, NJ) as described (Tatulian et al., 1998b). Small unilamellar vesicles, at a total lipid concentration of 200 μM, were obtained by sonication of the lipid suspension with a tip sonicator. Aliquots of stock PLA_2 solutions were added to the lipid suspension in a quartz cuvette to achieve desired PLA_2 concentrations. The lipid concentration was kept constant by adding appropriate amounts of the stock lipid sample. Binding of PLA_2 to vesicles resulted in energy transfer from the donor (the indole group of tryptophan) to the acceptor (the dansyl group of DPE) due to short-range dipole-dipole interactions.

Circular dichroism (CD) measurements were carried out on a Jasco J-720 spectropolarimeter (Jasco, Easton, MD) using a 0.05-cm path-length cuvette at ambient temperature. Sonicated vesicles were prepared at a total lipid concentration of 0.5 mM in a buffer that contained 0.5 mM EGTA and 10 mM Na-K-phosphate (pH 8.0).

PLA_2 activity was measured spectrophotometrically using the $sPLA_2$ activity kit from Cayman Chemical (Ann Arbor, MI). Hydrolysis of the *sn*-2 ester bond of diheptanoyl thiophosphatidylcholine by PLA_2 is followed by the exposure of free thiols, which triggers the conversion of 5,5′-dithio-*bis*-(2-nitrobenzoic acid) (DTNB) to 5-thio-nitrobenzoic acid that is detected by absorbance at 414 nm. The activity of PLA_2 toward supported lipid membranes was evaluated by ATR-FTIR based on the partial removal of the lipid-hydrolysis products from the membrane, as described (Tatulian, 2001). The spectra were recorded between 5 and 10 min after the addition of a given concentration of PLA_2, based on the fact that under conditions of ATR-FTIR experiments, the process of lipid removal saturates in ~5 min (see Fig. 5 in Tatulian, 2001). Protein concentration was measured by Bradford assay (Bradford, 1976).

Data analysis

The ATR-FTIR absorbance spectra are dominated by the signal from the supported membrane, including the membrane-bound protein, whereas the molecules far from the membrane do not contribute to the ATR-FTIR spectra (see Fig. 1 in Tatulian, 2001). This makes the ATR-FTIR spectroscopy a surface-sensitive technique that allows one to study protein binding to supported membranes, the enzymatic activity of PLA_2, and structural changes in both membrane lipids and the protein that result from protein-membrane interactions.

ATR-FTIR experiments on the membrane binding of PLA_2 were repeated three times and were reproducible. The number of PLA_2 molecules bound per unit area of the membrane was determined as $n = 2(P/L)/A$, where A is the cross-sectional area per lipid molecule and P/L is the bound protein-to-lipid molar ratio, which was determined as described (Tatulian, 2001). Values of $A = 68$ Å^2 have been used for both 1-palmitoyl-2-

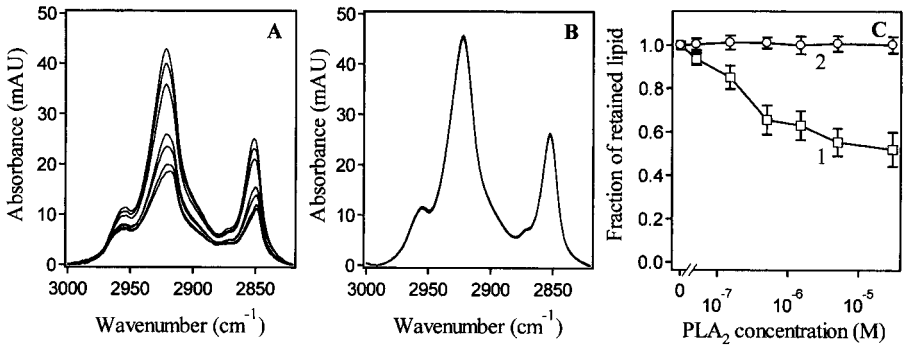

FIGURE 1 Effect of the native (*A*) and His^{48}-modified (*B*) PLA_2 enzymes on the lipid methylene stretching bands in supported membranes that contain POPC in the lower leaflet and POPC/POPG (4:1 ratio) in the upper leaflet. The ATR-FTIR spectra (*A* and *B*) correspond to PLA_2 concentrations of 0, 0.05, 0.15, 0.5, 1.5, 5, and 30 μM (from top to bottom). Panel *C* shows the dependence of the normalized intensities of the lipid methylene stretching bands on the concentrations of the native (*trace 1*) and His^{48}-modified (*trace 2*) PLA_2. The buffer contained (in mM) 100 NaCl, 15 KCl, 2 $CaCl_2$, 1 NaN_3, and 10 HEPES (pH 8.2).

oleoylphosphatidylcholine (POPC) and 1-palmitoyl-2-oleoylphosphatidylglycerol (POPG) (Seelig et al., 1993). The binding of PLA_2 to membranes was described using a Langmuir adsorption isotherm supplemented with the Hill cooperativity coefficient:

$$n = \frac{NC^{\alpha_H}K^{\alpha_H}}{1 + C^{\alpha_H}K^{\alpha_H}}, \quad (1)$$

where N is the number of binding sites per unit area, C is the PLA_2 concentration, K is the apparent binding constant, and α_H is the Hill coefficient. Values of N, K, and α_H were found from Scatchard plots as described (Tatulian, 2001).

The order parameter of the lipid acyl chains was determined by ATR-FTIR technique as $S_L = 2B/(3E_z^2 - B)$, where $B \equiv E_x^2 + E_z^2 - R^{ATR}E_y^2$; and E_x, E_y, and E_z are the orthogonal components of the electric vector of the evanescent field in the membrane (Fringeli, 1993).

The dynamic structures of the native and modified PLA_2s free in solution and bound to supported membranes were studied by analyzing the differences between the normalized amide I spectra of two samples at similar times of HX as described in more detail by Tatulian et al. (1998a).

Changes in the secondary structure of PLA_2 induced by membrane binding were evaluated by CD and FTIR techniques. Far-ultraviolet (UV) CD spectra of PLA_2 free in solution and in the presence of lipid vesicles were compared to reveal changes in the content and flexibility of α-helices upon binding of the enzyme to membranes. FTIR spectra of the free and membrane-bound enzymes were obtained by direct-transmission FTIR without polarization and by the ATR-FTIR technique at parallel and perpendicular polarizations, respectively. The second derivatives of direct-transmission spectra were calculated using the raw spectra. Before calculation of the second derivatives of the ATR-FTIR spectra of the membrane-bound protein, the spectra measured at parallel and perpendicular polarizations of the incident light (i.e., $A_\parallel$ and $A_\perp$) were used to obtain the total (i.e., polarization-independent) absorbance spectrum: $A = A_\parallel + GA_\perp$, where the scaling factor G is 0.78 under the present experimental conditions (Marsh, 1999). Likewise, the polarized ATR-FTIR spectra were corrected according to this procedure before calculation of the difference amide I spectra.

RESULTS

Effect of His^{48} modification on PLA_2 activity

PLA_2 activity against supported membranes was assessed by monitoring the PLA_2 concentration-dependent decreases in the lipid methylene stretching bands in the 3000–2820 cm^{-1} region (Tatulian, 2001). Action of the native PLA_2 on supported bilayers composed of POPC and POPG resulted in a dose-dependent decrease in the lipid methylene stretching bands (Fig. 1, *A* and *C*, *trace 1*). In contrast, the addition of increasing concentrations of His^{48}-modified PLA_2 to membranes of similar lipid composition had no effect on the lipid CH_2 bands, demonstrating complete inhibition of the enzyme activity by bromophenacylation (Fig. 1, *B* and *C*, *trace 2*). Inactivation of pBPB-treated PLA_2 was also demonstrated by diheptanoyl thiophosphatidylcholine/DTNB assay (not shown). Inhibition of secretory PLA_2s by pBPB is in agreement with our earlier results on the same PLA_2 isoform, AppD49 (Tatulian et al., 1998b), as well as with the data obtained for PLA_2s from porcine pancreas (Volwerk et al., 1974) or from snake venom (Halpert et al., 1976; Yang and King, 1980).

Membrane binding of native and His^{48}-modified PLA_2s

Binding of PLA_2 to lipid vesicles and to supported bilayers was measured, respectively, by NET and by ATR-FTIR spectroscopy. The data of Fig. 2 show that under noncatalytic conditions (0.5 mM EGTA), the efficiency of energy transfer from both the native and covalently inhibited PLA_2s to membranes composed of POPC and 10% DPE significantly increases when the membranes contain 20 mol % negatively changed lipid, POPG. This is consistent with previous findings indicating stronger binding of group I/II PLA_2s to membranes with increased negative surface potential (Gelb et al., 1995, 1999; Han et al., 1997; Tatulian, 2001). It was shown earlier that DPE does not specifically interact with secretory PLA_2s (Jain and Vaz, 1987). Therefore, binding of PLA_2 to vesicles is not likely to be strongly modulated by the presence of DPE. Despite this, the results of NET experiments have not been used for quantitative characterization of PLA_2-membrane interactions and for comparison of membrane binding of the native and inhibited PLA_2s, because the bromophenacylated PLA_2 partially quenched the fluorescence emission, which was probably due to the presence of bromine in modified PLA_2 samples (Fig. 2).

The binding of the native and pBPB-modified PLA_2s to supported membranes that contained POPC in the lower

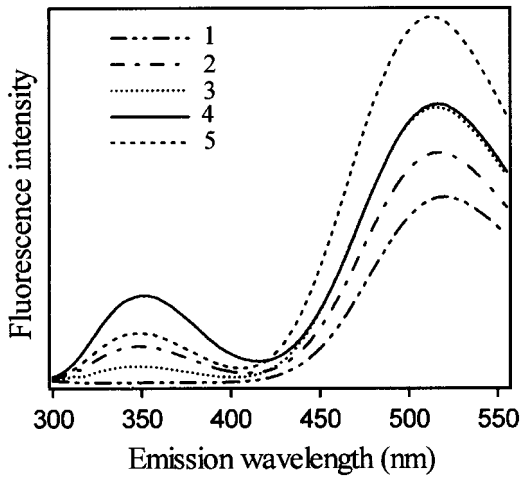

FIGURE 2 Fluorescence emission spectra of lipid vesicles composed of 90% POPC and 10% DPE (*traces 1, 2*, and *4*) or 70% POPC, 20% POPG, and 10% DPE (*traces 3* and *5*) in the absence (*trace 1*) or presence (*traces 4* and *5*) of 3 μM native or His^{48}-modified PLA_2 (*traces 2* and *3*). Excitation was at 284 nm. Fluorescence emission bands around ~350 and ~510 nm are generated by tryptophan and dansyl groups, respectively. Note energy transfer from the tryptophans of PLA_2 to the dansyl group of DPE in vesicle membranes, indicating binding of the enzyme to membranes. The buffer contained (in mM) 100 NaCl, 15 KCl, 1 NaN_3, 0.5 EGTA, and 10 HEPES (pH 8.2).

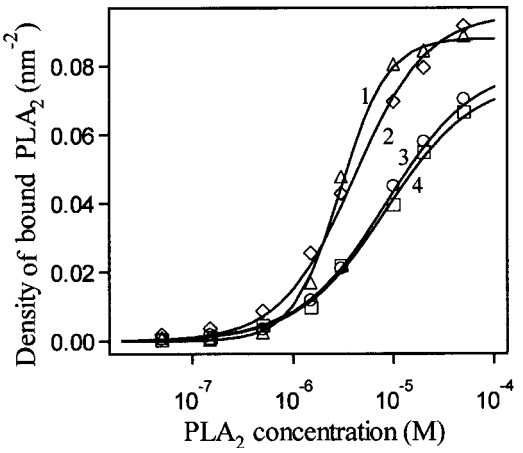

FIGURE 3 Binding of the native (△ and ◇) and His^{48}-modified PLA_2 (○ and □) to supported membranes that contain POPC in the lower leaflet and POPC/POPG (4:1 ratio) in the upper leaflet. The buffer contained (in mM) 100 NaCl, 15 KCl, 1 NaN_3, and 10 HEPES (pH 8.2) plus 0.5 EGTA (○ and ◇) or 2 $CaCl_2$ (△ and □). The curves were simulated using Eq. 1 with the following parameters: trace 1, $K = 3.4 \times 10^5\ M^{-1}$, $N = 0.088\ nm^{-2}$, $\alpha_H = 1.86$; trace 2, $2.5 \times 10^5\ M^{-1}$, $N = 0.095\ nm^{-2}$, $\alpha_H = 1.2$; trace 3, $K = 1.2 \times 10^5\ M^{-1}$, $N = 0.08\ nm^{-2}$, $\alpha_H = 1.0$; and trace 4, $K = 1.2 \times 10^5\ M^{-1}$, $N = 0.076\ nm^{-2}$, $\alpha_H = 1.0$. The standard deviations from the average data points were typically 5–15% and are not shown for the sake of clarity.

leaflet and a POPC/POPG (4:1) mixture in the upper leaflet was measured by ATR-FTIR both in the absence of free Ca^{2+} (0.5 mM EGTA) and in the presence of 2 mM $CaCl_2$. In the absence of Ca^{2+}, i.e., under conditions that prevent lipid hydrolysis by the native enzyme, the experimental data were fitted by Eq. 1 using $K = 2.5 \times 10^5\ M^{-1}$, $N = 0.095\ nm^{-2}$, and $\alpha_H = 1.2$ for the native PLA_2 and $K = 1.2 \times 10^5\ M^{-1}$, $N = 0.08\ nm^{-2}$, and $\alpha_H = 1.0$ for the inhibited enzyme (Fig. 3). In the presence of 2 mM $CaCl_2$, the binding of the native PLA_2 was characterized by $K = 3.4 \times 10^5\ M^{-1}$, $N = 0.088\ nm^{-2}$, and $\alpha_H = 1.86$, whereas the parameters for the inhibited PLA_2 were $K = 1.2 \times 10^5\ M^{-1}$, $N = 0.076\ nm^{-2}$, and $\alpha_H = 1$. Note that the binding parameters were determined independently using two types of Scatchard plots as described by Tatulian (2001). These data indicate that 1). in the presence of Ca^{2+} (which supports catalysis), the binding constant of the native PLA_2 moderately increases, the binding-site density decreases, and PLA_2-membrane interaction becomes more cooperative; and 2). membrane binding of pBPB-inhibited PLA_2 is weaker and noncooperative compared to that of the native PLA_2 and exhibits little dependence on Ca^{2+}. Although distinct differences were detected between the membrane-binding parameters of the native PLA_2 in the presence and absence of Ca^{2+}, these changes in membrane-binding characteristics were clearly not as significant as those caused by His^{48} modification of PLA_2. These results suggest that factors other than removal of the protein-bound Ca^{2+} ion, probably involving conformational changes in the protein, are responsible for the impaired membrane binding of His^{48}-modified PLA_2.

Effects of PLA_2 on membrane structure

The physical state of membranes is an important determinant of the activity of membrane-bound PLA_2 (Gelb et al., 1995, 1999; Burack and Biltonen, 1994; Burack et al., 1997; Berg et al., 2001; Tatulian, 2001). Lipid hydrolysis and dissociation of a fraction of reaction products from the membrane significantly modulate the membrane structure and thereby affect PLA_2 activity. Therefore, for the understanding of the reciprocal mechanisms involved in the interfacial activation of PLA_2, it is important to examine the effects of PLA_2 on the membrane structure. The structural effects of PLA_2 on both the interfacial headgroup region and the hydrocarbon core of phospholipid membranes are described below.

Lipid polar headgroup region

Addition of the native PLA_2 to supported membranes under both catalytic and noncatalytic conditions (i.e., in the presence and absence of Ca^{2+}) resulted in a decrease in the frequency of the lipid carbonyl stretching band. The second-derivative spectra revealed two components at ~1742 and ~1728 cm^{-1}, a pattern that was observed previously for diacyl phosphatidylcholines in aqueous media (Blume et al., 1988). Data obtained under catalytic conditions, i.e., in the presence of 2 mM $CaCl_2$, are presented in Fig. 4. With increasing concentration of native PLA_2, the relative intensity of the lower frequency component increased while that of the higher frequency component decreased, resulting in a shift of the whole C=O band toward lower frequencies.

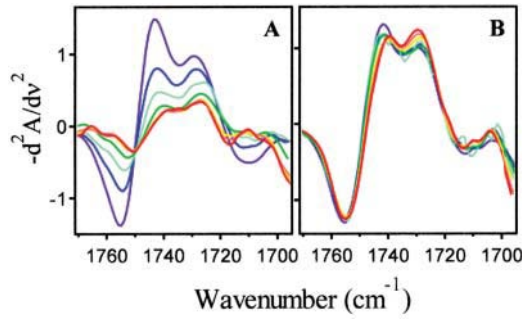

FIGURE 4 Second-derivative ATR-FTIR spectra of supported membranes that initially contained POPC in the lower leaflet and POPC/POPG (4:1 ratio) in the upper leaflet. The change of the color code from purple to red indicates a change in the concentration of the native (*A*) and His^{48}-modified (*B*) PLA_2 from 0 to 30 μM. The buffer contained (in mM) 100 NaCl, 15 KCl, 1 NaN_3, 2 $CaCl_2$, and 10 HEPES (pH 8.2).

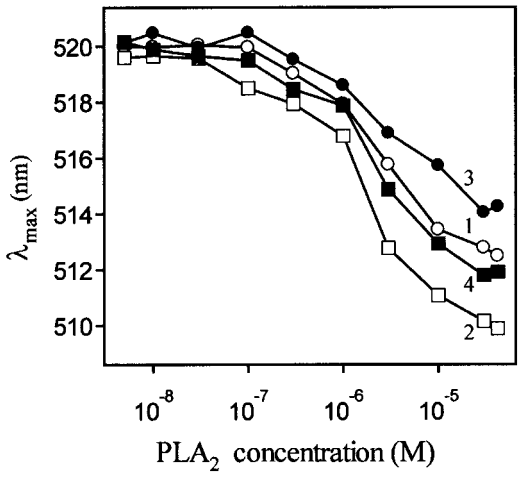

FIGURE 5 Maximum wavelength (λ_{max}) of DPE (energy acceptor) fluorescence emission as a function of the native (*traces 1* and *2*) and His^{48}-modified (*traces 3* and *4*) PLA_2 concentration as derived from the experiments described in Fig. 2. The vesicles were composed of 90% POPC and 10% DPE (*traces 1* and *3*) or 70% POPC, 20% POPG, and 10% DPE (*traces 2* and *4*).

The bromophenacylated PLA_2 exerts a much weaker effect on the lipid carbonyl band. Similar results were obtained under noncatalytic conditions, i.e., in the presence of 0.5 mM EGTA (not shown).

Infrared vibrational frequencies are proportional to the square root of the force-field constants of corresponding vibrational modes. On the other hand, the strength of a covalent bond decreases upon hydrogen bonding of one or both participating atoms, predicting a lower stretching frequency for hydrogen-bonded C=O groups. Indeed, the carbonyl-stretching band components of membrane lipids at ~1742 and ~1728 cm^{-1} were shown to represent C=O groups that are, respectively, dehydrated or hydrogen bonded to water (Blume et al., 1988). Therefore, an increase in the ratio of intensities A_{1728}/A_{1742} indicates a PLA_2 concentration-dependent increase in the fraction of hydrogen-bonded lipid carbonyl groups. In the presence of PLA_2, the lipid C=O groups could form hydrogen bonds either with water or with membrane-bound PLA_2. To determine whether the increase in the relative intensity of the component at 1728 cm^{-1} results from hydrogen bonding of the lipid with water or with PLA_2, the effect of PLA_2 on membrane hydration was determined based on the spectral shifts of DPE fluorescence as a function of PLA_2 concentration. The fluorescence emission frequency of the dansyl chromophore of DPE increases as its microenvironment becomes less polar, or when the polar solvent (water) is removed from the membrane surface (Jain and Vaz, 1987; Lakowicz, 1999). A significant blue shift was detected in the DPE fluorescence with increasing PLA_2 concentration, indicating a reduction of the polarity of the membrane surface (Figs. 2 and 5). The most straightforward interpretation of this effect is membrane dehydration as a result of PLA_2 binding. Binding of either the native or the modified PLA_2 to vesicles caused a considerably larger blue shift of DPE fluorescence when the membranes contained 20 mol % acidic lipid, POPG, and the effect induced by the native PLA_2 was stronger than that of the modified PLA_2 (Fig. 5), indicating a correlation between the strength of membrane binding of PLA_2 and membrane dehydration. An increase in the hydrogen bonding of the lipid carbonyl groups (Fig. 4) and a reduced hydration of the membrane surface with increasing PLA_2 concentration (Fig. 5) suggest that PLA_2 binding to the membranes results in membrane dehydration and formation of PLA_2-membrane hydrogen bonding. Data presented in Figs. 2, 3, 4, and 5 indicate that His^{48} modification results in a weaker membrane binding of PLA_2 and an impairment in the ability of the enzyme to dehydrate the membrane surface and to form hydrogen bonding with membrane lipids.

Lipid hydrocarbon chain region

The effect of the native and modified PLA_2 on the conformation of hydrocarbon chains of lipids was monitored by ATR-FTIR spectroscopy. It is known that a transition of lipids from the well-ordered gel state to the more disordered liquid-crystalline state is accompanied by 1), an increase in the methylene stretching frequencies, 2), a broadening of the corresponding absorbance bands, and 3), a decrease in the acyl chain order parameter (Mendelsohn and Mantsch, 1986; Mantsch and McElhaney, 1991). ATR-FTIR experiments revealed that the lipid methylene stretching frequencies were higher and the order parameters were lower for membranes composed of POPC and POPG as compared with membranes composed of DPPC and DPPG, indicating more ordered packing of lipids with saturated acyl chains. Interestingly, the CH_2 stretching frequencies of POPC/POPG membranes decreased and the order parameter increased as a function of the concentration of native PLA_2, whereas the opposite effect was observed for DPPC/DPPG membranes (Fig. 6). These data imply that under

catalytic conditions, the native PLA_2 increases the order of membranes in the fluid phase but induces more disorder in the gel-phase membranes. Inhibition of PLA_2 by EGTA only accentuated the ordering effect of the enzyme on POPC/POPG membranes as judged from a steeper decrease in the methylene stretching frequencies and an increase in the order parameter as a function of PLA_2 concentration (Fig. 6). On the other hand, the disordering effect of the native PLA_2 on DPPC/DPPG membranes is more moderate when free Ca^{2+} is removed by EGTA (data not shown). A common effect accompanying lipid hydrolysis by PLA_2, i.e., a broadening of methylene stretching bands, was observed for both POPC/POPG and DPPC/DPPG membranes, implying that in both cases, a component with increased motional flexibility of lipid acyl chains is involved. Finally, PLA_2 that was inhibited by bromophenacylation of His^{48} did not have any significant effects on the structure of either POPC/POPG or DPPC/DPPG membranes (Fig. 6, *insets*).

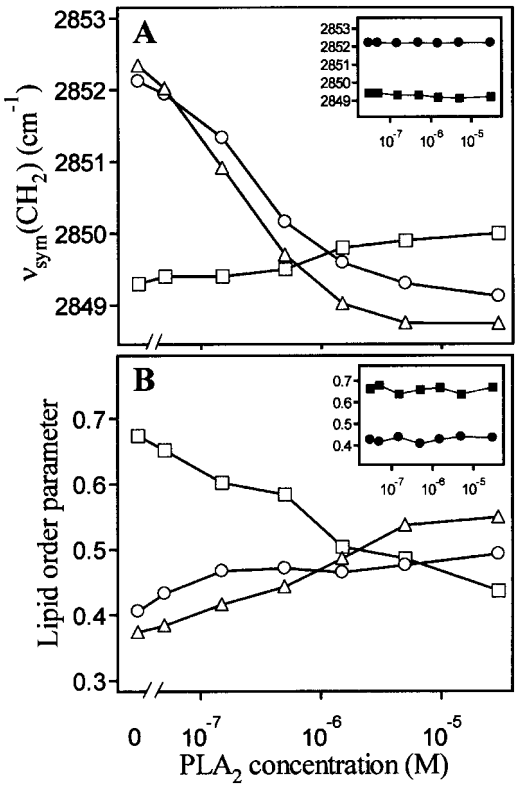

FIGURE 6 Dependence of the lipid symmetric methylene stretching frequency (ν_{sym}; *A*) and the lipid acyl chain order parameter (*B*) on the native (*open symbols*) and His^{48}-modified PLA_2 concentration (*closed symbols*, *insets*) obtained by ATR-FTIR experiments. Circles and triangles correspond to membranes containing POPC in the lower leaflet of the supported membranes and a 4:1 mixture of POPC/POPG in the upper leaflet, whereas squares correspond to membranes composed of DPPC in the lower leaflet and a 4:1 mixture of DPPC/DPPG in the upper leaflet. The buffer contained (in mM) 100 NaCl, 15 KCl, 1 NaN_3, and 10 HEPES (pH 8.2) plus 0.5 mM EGTA (△) or 2 mM $CaCl_2$ (○, ●, and □, ■).

These data suggest a complex nature of the influence of PLA_2 on the structure of membrane lipids, involving both ordering and disordering effects. PLA_2 probably modulates the lipid structure by a dual mechanism: binding of PLA_2 to the membrane surface, by itself, makes the membrane more ordered (primary effect), whereas lipid hydrolysis perturbs the membrane structure (secondary effect). Recent electron paramagnetic resonance spectroscopy data on the effect of PLA_2 on membrane structure have been interpreted in a similar manner (Tatulian, 2002).

Effects of membrane binding on the structure of the native and His^{48}-modified PLA_2

Previous studies indicated that the interfacial activation of PLA_2 by binding to the membrane surface is accompanied by structural changes in the enzyme, i.e., induction of α-helices with increased flexibility (Tatulian et al., 1997; Tatulian, 2001). CD and FTIR results (including amide HX) presented here identify distinct conformational effects in both the native and His^{48}-modified PLA_2 that are induced by membrane binding.

CD data

CD experiments revealed typical α-helical spectra with double minima at ~210 and ~224 nm for both the native and His^{48}-modified PLA_2s. The mean residue molar ellipticity (symbolized by $[\theta]$) of the modified enzyme was more negative in this region, indicating an increased α-helical content in the His^{48}-modified PLA_2 (Fig. 7). Binding of the native PLA_2 to vesicles resulted in more negative $[\theta]$ values, indicating an increase in the α-helical content, but this effect was weaker for the modified enzyme. Distinct differences in the shapes of CD spectra of the native and modified proteins have been revealed: the ratio $[\theta]_{222}/[\theta]_{211}$ was higher for the modified than the native PLA_2 (Figs. 7 and 8). Also, the parallel $\pi\pi^*$ exciton band, which occurs at ~208 nm in normal α-helices, was red-shifted in the spectrum of the modified enzyme. Both the increased $[\theta]_{222}/[\theta]_{211}$ ellipticity ratio and the red-shifted $\pi\pi^*$ transition indicate helices with decreased rigidity (Cooper and Woody, 1990; Zhou et al., 1992; Graddis et al., 1993). Therefore, the CD data suggest an increased level of more flexible α-helices in the modified PLA_2. This conclusion was confirmed by FTIR and amide HX experiments.

FTIR data

Earlier studies identified a splitting of the α-helical component of the amide I band of the native PLA_2 upon membrane binding (Tatulian et al., 1997). In addition to the component at ~1650 cm^{-1}, a new component at ~1658 cm^{-1} appeared in the membrane-bound enzyme that was ascribed to a more flexible α-helical structure, possibly an

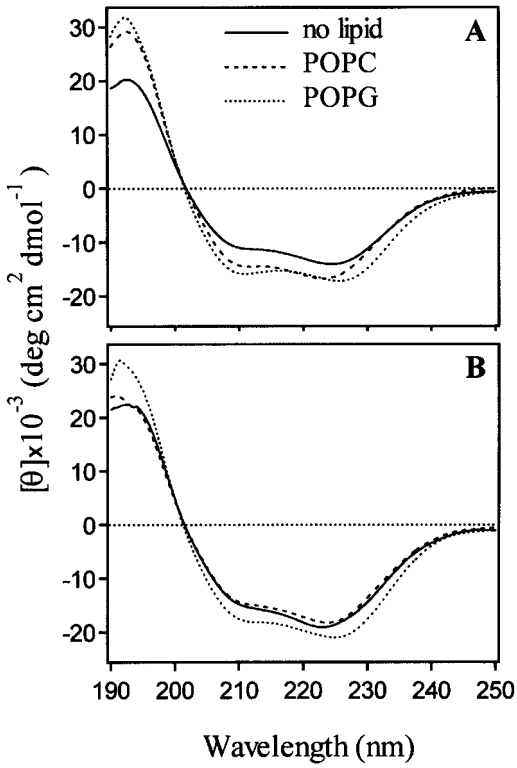

FIGURE 7 Circular dichroism spectra of the native (*A*) and His^{48}-modified (*B*) PLA_2 free in solution and in the presence of sonicated POPC or POPG vesicles, as indicated. Spectra were also measured in the presence of vesicles composed of POPC and POPG at varying proportions; some characteristics of those spectra are shown in Fig. 8. The buffer contained 0.5 mM EGTA and 10 mM Na-K-phosphate (pH 8.0).

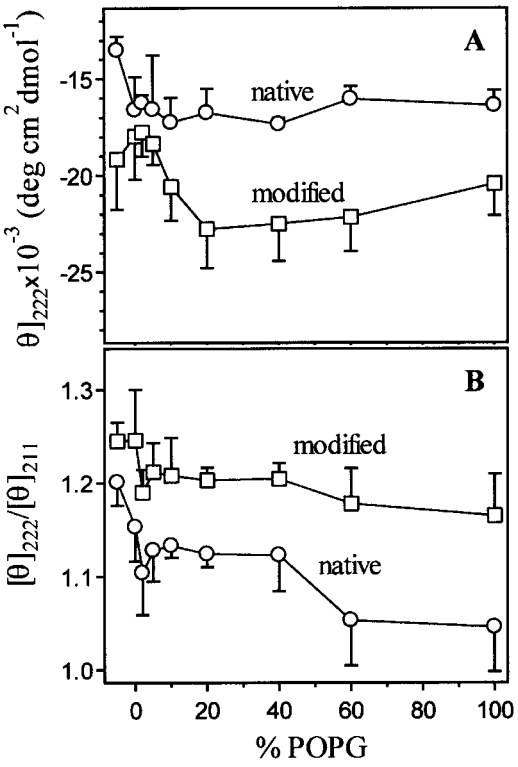

FIGURE 8 The mean residue molar ellipticities at 222 nm (*A*) and the ratios of ellipticities at 222 and 211 nm (*B*) as functions of the mol % of POPG in POPC/POPG mixed vesicles for both the native and His^{48}-modified PLA_2s, as indicated. These data were derived from the CD experiments described in Fig. 7. The data for values of % POPG < 0 correspond to the absence of lipid in the PLA_2 sample.

α_{II}-helix. The resolution-enhanced (second derivative) amide I spectra of the His^{48}-modified enzyme revealed a split signal in the α-helical region that comprised two components at $\sim$1656 and $\sim$1649 cm^{-1} both in solution and in the membrane-bound state (Fig. 9). These data imply that less-stable helices with increased amide I frequencies are present in the modified PLA_2, and membrane binding exerts little effect on its structure. Analysis of the amide I bands of the native and modified enzymes indicated higher α-helical content in the modified protein, which is consistent with the CD studies described above. Altogether, CD and FTIR experiments suggest that the modified PLA_2 contains a larger fraction of α-helix that is characterized by decreased stability. Although the native PLA_2 acquires more dynamic properties upon membrane binding, the structure of the modified enzyme is not significantly affected by interactions with membranes.

Amide hydrogen exchange data

To directly assess the changes in the dynamic structures of both the native and inhibited PLA_2s upon membrane binding, amide HX was measured for both forms of PLA_2 using FTIR spectroscopy. The HX can be measured by observing the shift of the amide I band toward lower frequencies after exposing the sample to D_2O (Tatulian et al., 1997; Tatulian et al., 1998a,b). The difference spectra of amide I bands at similar time points of deuteration directly indicate differences in the dynamic structure of the protein in the two samples. The difference spectra between the free and membrane-bound native PLA_2 show that before the initiation of HX, the amide I band of the membrane-bound enzyme occurs at higher frequencies; but in the course of HX, shifts toward lower frequencies much more extensively than that of the free enzyme, reflecting an increase in the flexibility of PLA_2 structure upon membrane binding (Fig. 10 *A*). Similar difference spectra of the His^{48}-modified PLA_2 indicate little spectral shifts in the course of deuteration for both free and membrane-bound forms of the inhibited enzyme (Fig. 10 *B*). Finally, the difference spectra of membrane-bound native minus modified PLA_2s indicate that the amide I band of the native PLA_2 progressively moves from higher to lower frequencies, whereas the modified enzyme shows little spectral shifts (Fig. 10 *C*). Together, CD and FTIR results (including HX experiments) imply that during interfacial activation via membrane binding, the native PLA_2 molecule acquires more dynamic properties, which presumably confer plasticity to the enzyme that is required for the multistep

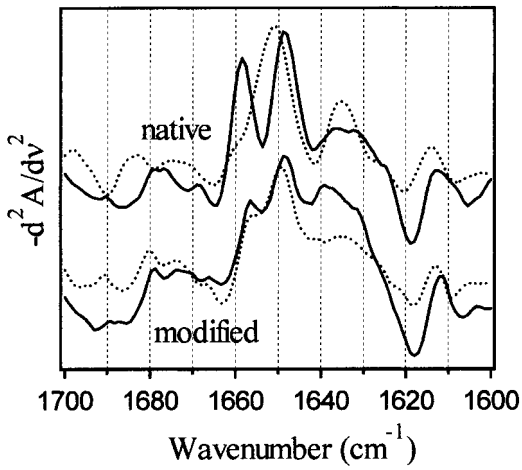

FIGURE 9 Second-derivative amide I spectra of the native and His^{48}-modified PLA_2 free in solution (*dotted lines*) and bound to POPC/POPG (4:1 ratio)-supported membranes (*solid lines*) measured, respectively, by direct-transmission and ATR-FTIR techniques. The buffer contained (in mM) 100 NaCl, 15 KCl, 2 $CaCl_2$, 1 NaN_3, and 10 HEPES (pH 8.2).

catalytic process. The covalently inhibited PLA_2 is probably arrested in some intermediate conformation that is not affected by membrane binding.

DISCUSSION

Because of initial indications that pBPB is an active site-directed inhibitor of PLA_2 rather than a general histidine modifier (Volwerk et al., 1974; Halpert et al., 1976; Yang and King, 1980), this compound attracted substantial interest as an efficient tool for pharmacological and mechanistic studies on PLA_2s. The crystal structure of His^{48}-bromophenacylated PLA_2 from the venom of *A. h. pallas* (PDB access code: 1bk9) shows the pBPB moiety embedded in the substrate-binding pocket in a way that completely blocks the access of the substrate to the catalytic site of the enzyme. In addition to blockage of the substrate access and abolition of the general base function of His^{48}, bromophenacylation results in the displacement of the catalytic water molecule(s), impairment of Ca^{2+} binding, and distortion of the hydrogen-bonding network that maintains the structural integrity of the enzyme (Halpert et al., 1976; Yang and King, 1980; Renetseder et al., 1988; Zhao et al., 1998). The present results imply that modification of the catalytic His^{48} residue of PLA_2 not only inhibits the enzyme, but also exerts significant effects on its dynamic structure and membrane-binding properties, suggesting that the membrane-binding surface acts as a regulatory site and is structurally coupled to the catalytic center of PLA_2.

The presence of Ca^{2+} ions increases the apparent binding constant and binding cooperativity of native PLA_2 for negatively charged membranes and decreases the binding-site density. Calcium could affect membrane binding of PLA_2 by diverse mechanisms. First, Ca^{2+} activates PLA_2 as a mandatory cofactor, resulting in accumulation of phospholipid hydrolysis products in the membrane that have been shown to increase the affinity of PLA_2 for membranes (Jain et al., 1982; Jain and de Haas, 1983; Bayburt et al., 1993; Burack et al., 1997). Second, binding of Ca^{2+} to PLA_2 may increase its cationic charge and thereby increase its binding constant for negatively charged membranes. Third, Ca^{2+}-dependent changes in the structure of PLA_2 (Scott and Sigler, 1994b) may affect the binding constant and cooperativity of PLA_2-membrane interactions. The increase in PLA_2 binding-site density after the removal of Ca^{2+} by EGTA may be explained in terms of a competition between Ca^{2+} and PLA_2 for negatively charged lipids in the membrane. Calculations using previously evaluated parameters of Ca^{2+} binding to acidic lipids (Tatulian, 1995) indicated that 2 mM Ca^{2+} could neutralize ~40% of the acidic lipid in the membrane. In the presence of PLA_2, however, 2 mM Ca^{2+} decreases N by only ~8%, probably because PLA_2 competitively removes most of the membrane-bound Ca^{2+} from the membrane surface.

His^{48} bromophenacylation of PLA_2 impairs its membrane-binding capabilities (Figs. 2 and 3). Displacement of the Ca^{2+} ion by pBPB modification of PLA_2 (Renetseder et al., 1988; Zhao et al., 1998) and subsequent reduction of the effective cationic charge of the enzyme is not likely to account for this effect. Significant difference between the effects of EGTA and pBPB on the membrane binding of

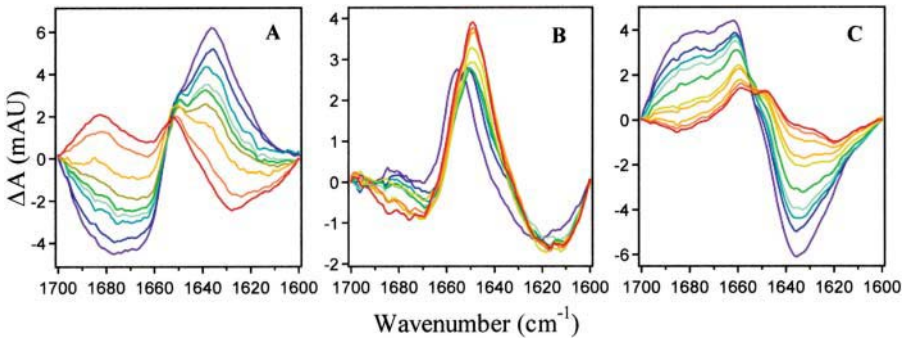

FIGURE 10 FTIR difference spectra in the amide I region, revealing differences in the dynamic structures of the native and His^{48}-modified PLA_2s free in solution and bound to supported membranes. (*A*) The difference between the spectra of free and membrane-bound native PLA_2. (*B*) Difference between the spectra of free and membrane-bound His^{48}-modified PLA_2. (*C*) Difference between the membrane-bound native and modified PLA_2s. The spectra of PLA_2 free in solution and bound to supported membranes composed of POPC and POPG (4:1 ratio) were measured by direct-transmission and ATR-FTIR techniques, respectively. The change of color code from purple to red corresponds to an increase in the hydrogen exchange time from 2 to 1220 min. The buffer contained (in mM) 100 NaCl, 15 KCl, 1 NaN_3, 0.5 EGTA, and 10 HEPES (pH 8.2).

PLA_2 indicates that PLA_2 modification by pBPB has more complex consequences than simply removing the Ca^{2+} ion. The His^{48}-attached pBPB is hidden in the substrate-binding pocket and is relatively far from the putative membrane-binding residues (see PDB file 1bk9); it cannot make a direct contact with the membrane and thereby modulate the membrane binding of PLA_2. These considerations lead to a conclusion that the effect of covalent modification of PLA_2 on its membrane-binding properties probably results from conformational changes in the protein that extend from the catalytic site to the membrane-binding surface of PLA_2. CD and FTIR data discussed below provide support for this conclusion.

Significant differences between the far-UV CD spectra of the native and modified PLA_2s (increased ratio of ellipticities at 222 and 211 nm in the latter case; see Figs. 7 and 8) suggest that α-helices of His^{48}-modified PLA_2 are more flexible and undergo smaller structural changes upon membrane binding as compared to the native enzyme. Furthermore, FTIR experiments indicate that membrane binding of the native PLA_2 results in the appearance of an additional α-helical component at higher frequencies (Fig. 9) that has been attributed to a more flexible helical structure with weaker hydrogen bonding (Tatulian et al., 1997; Tatulian, 2001). An increase in the flexibility of the native PLA_2 structure upon membrane binding is confirmed by amide HX data (Fig. 10). In conjunction with the results of Figs. 4 and 5, which suggest PLA_2-induced dehydration of the membrane surface and formation of PLA_2-membrane hydrogen bonding, these data imply that modification of the helices of PLA_2 upon membrane binding may (partially) result from hydrogen bonding between membrane lipids and the backbone atoms of α-helices of PLA_2. Interestingly, high-resolution structures of both mature and pro-PLA_2 crystallized in the presence of sulfate or phosphate anions (which mimic the anionic charge of the membrane surface) indicated hydrogen bonding between the *backbone* amide groups of PLA_2 and the oxyanions (Pan et al., 2001; Epstein et al., 2001), which provides additional support for this conclusion. Removal of membrane-bound water is likely to favor PLA_2-membrane interactions not only by allowing PLA_2 to form hydrogen bonds with membrane lipids, but also by decreasing the free energy of the system through the entropic factor. PLA_2-membrane hydrogen bonding at the expense of helical hydrogen bonds of PLA_2 will stabilize PLA_2-membrane interactions and, at the same time, impart conformational flexibility to the enzyme. Both stronger PLA_2-membrane interactions and increased plasticity of the enzyme are probably required for efficient lipolysis, i.e., lipid binding, hydrolysis, and release of the products.

Next, the α-helical signal of the His^{48}-modified PLA_2 is split both in solution and in the membrane-bound state, but the higher frequency component is weaker and is slightly red-shifted as compared to that in the spectrum of the membrane-bound native PLA_2 (Fig. 9). This means that His^{48} bromopheacylation of PLA_2 destabilizes the helices of the protein. However, the structure of the modified PLA_2 is not influenced by membrane binding. Amide HX experiments support this conclusion by indicating that 1) upon membrane binding, the structure of the native PLA_2 becomes more flexible, whereas that of the modified PLA_2 does not change; and 2) the structure of the membrane-bound native PLA_2 is more flexible than that of the membrane-bound modified PLA_2 (Fig. 10).

Comparison of the crystal structures of native and pBPB-modified bovine pancreatic PLA_2s indicates that the distance between the Nε2 atom of His^{48} and the side-chain carboxyl oxygen of Asp^{99} (Oδ1 in the orthorhombic form and Oδ2 in the trigonal form) increases by 0.47 Å upon pBPB modification, which is enough for disruption of the His^{48}-Asp^{99} hydrogen bonding that is crucial in both structural and functional terms (see PDB files 1bp2 and 2bpp). This is likely to decrease the structural stability of PLA_2, which is confirmed by the present data. Conformational effects accompanying the interfacial activation of PLA_2 evidently involve destabilization of α-helices. These structural changes do not occur upon membrane binding of the His^{48}-modified enzyme, probably because pBPB has already distorted the structural elements determining the interfacial activation competence of the enzyme. Finally, these results indicate a coupling between the catalytic and membrane-binding sites of secretory PLA_2s. Structural effects caused by the modification of a catalytic residue are reflected at the membrane-binding surface, which acts as a regulatory site of the enzyme and uses the same coupling mechanisms to transmit membrane-induced structural changes to the catalytic center in the process of interfacial activation of PLA_2.

The PDB file for the pBPB-modified bovine pancreatic PLA_2 was kindly provided by Prof. Bauke Dijkstra (University of Groningen). Purification of the native PLA_2 and its modification with pBPB in Prof. Rodney L. Biltonen's lab is gratefully acknowledged.

This work was supported by National Institutes of Health (HL-65524).

REFERENCES

Baker, S. F., R. Othman, and D. C. Wilton. 1998. Tryptophan-containing mutant of human (group IIa) secreted phospholipase A_2 has a dramatically increased ability to hydrolyze phosphatidylcholine vesicles and cell membranes. *Biochemistry*. 37:13203–13211.

Bayburt, T., B.-Z. Yu, H.-K. Lin, J. Browning, M. K. Jain, and M. H. Gelb. 1993. Human nonpancreatic secretory phospholipase A_2: interfacial parameters, substrate specificity, and competitive inhibitors. *Biochemistry*. 32:573–582.

Berg, O. G., M. H. Gelb, M.-D. Tsai, and M. K. Jain. 2001. Interfacial enzymology: the secreted phospholipase A_2-paradigm. *Chem. Rev.* 101:2613–2653.

Bezzine, S., R. S. Koduri, E. Valentin, M. Murakami, I. Kudo, F. Ghomashchi, M. Sadilek, G. Lambeau, and M. H. Gelb. 2000. Exogenously added human group X-secreted phospholipase A_2 but not the group IB, IIA, and V enzymes efficiently release arachidonic acid from adherent mammalian cells. *J. Biol. Chem.* 275:3179–3191.

Blume, A., W. Hübner, and G. Messner. 1988. Fourier transform infrared spectroscopy of $^{13}C{=}O$-labeled phospholipids. Hydrogen bonding to carbonyl groups. *Biochemistry*. 27:8239–8249.

Bradford, M. M. 1976. A rapid and sensitive method for the quantitation of microgram quantities of protein utilizing the principle of protein-dye binding. *Anal. Biochem*. 72:248–254.

Burack, W. R. and R. L. Biltonen. 1994. Lipid bilayer heterogeneities and modulation of phospholipase A_2 activity. *Chem. Phys. Lipids*. 73:209–222.

Burack, W. R., A. R. G. Dibble, M. M. Allietta, and R. L. Biltonen. 1997. Changes in vesicle morphology induced by lateral phase separation modulate phospholipase A_2 activity. *Biochemistry*. 36:10551–10557.

Cho, W. and Z. Shen. 1999. Efficient immobilization of phospholipase A_2. *In* Lipase and Phospholipase Protocols. M. Doolittle and K. Reue, editors. Humana Press, Totowa, NJ. 303–307.

Cooper, T. M. and R. W. Woody. 1990. The effect of conformation on the CD of interacting helices: a theoretical study of tropomyosin. *Biopolymers*. 30:657–676.

Epstein, T. M., B.-Z. Yu, Y. H. Pan, S. P. Tutton, B. P. Maliwal, M. K. Jain, and B. J. Bahnson. 2001. The basis for k_{cat}* impairment in phospholipases A_2 from the anion-assisted dimer structure. *Biochemistry*. 40:11411–11422.

Fringeli, U. P. 1993 In situ infrared attenuated total reflection membrane spectroscopy. *In* Internal Reflection Spectroscopy. Theory and Application. F. M. Mirabella, Jr., editor. Marcel Dekker, New York. 255–324.

Gelb, M. H., W. Cho, and D. C. Wilton. 1999. Interfacial binding of secreted phospholipases A_2: more than electrostatics and a major role for tryptophan. *Curr. Opin. Struct. Biol*. 9:428–432.

Gelb, M. H., M. K. Jain, A. M. Hanel, and O. G. Berg. 1995. Interfacial enzymology of glycerolipid hydrolysis: lessons from secretory phospholipase A_2. *Annu. Rev. Biochem*. 64:653–688.

Graddis, T. J., D. G. Myszka, and I. M. Chaiken. 1993. Controlled formation of model homo- and heterodimer coiled coil polypeptides. *Biochemistry*. 32:12664–12671.

Halpert, J., D. Eaker, and E. Karlsson. 1976. The role of phospholipase activity in the action of a presynaptic neurotoxin from the venom of *Notechis scutatus scutatus* (Australian tiger snake). *FEBS Lett*. 61:72–76.

Han, S. K., E. T. Yoon, D. L. Scott, P. B. Sigler, and W. Cho. 1997. Structural aspects of interfacial adsorption. A crystallographic and site-directed mutagenesis study of the phospholipase A_2 from the venom of *Agkistrodon piscivorus piscivorus*. *J. Biol. Chem*. 272:3573–3582.

Jain, M. K. and O. G. Berg. 1989. The kinetics of interfacial catalysis by phospholipase A_2 and regulation of interfacial activation: hopping versus scooting. *Biochim. Biophys. Acta*. 1002:127–156.

Jain, M. K., M. R. Egmond, H. M. Verheij, R. Apitz-Castro, R. Dijkman, and G. H. de Haas. 1982. Interaction of phospholipase A_2 and phospholipid bilayers. *Biochim. Biophys. Acta*. 688:341–348.

Jain, M. K. and G. H. de Haas. 1983. Activation of phospholipase A_2 by freshly added lysophospholipids. *Biochim. Biophys. Acta*. 736:157–162.

Jain, M. K. and W. L. C. Vaz. 1987. Dehydration of the lipid-protein microinterface on binding of phospholipase A_2 to lipid bilayers. *Biochim. Biophys. Acta*. 905:1–8.

Lakowicz, J. K. 1999. Principles of Fluorescence Spectroscopy. Kluwer Academic/Plenum Publishers, New York.

Li, Y. and M.-D. Tsai. 1993. Phospholipase A_2 engineering. 10. The aspartate. . .histidine catalytic diad also plays an important structural role. *J. Am. Chem. Soc*. 115:8523–8526.

Liu, X., H. Zhu, B. Huang, J. Rogers, B.-Z. Yu, A. Kumar, M. K. Jain, M. Sundaralingam, and M.-D. Tsai. 1995. Phospholipases A_2 engineering. Probing the structural and functional roles of N-terminal residues with site-directed mutagenesis, x-ray, and NMR. *Biochemistry*. 34:7322–7334.

Mantsch, H. H. and R. N. McElhaney. 1991. Phospholipid phase transitions in model and biological membranes as studied by infrared spectroscopy. *Chem. Phys. Lipids*. 57:213–226.

Maraganore, J. M., G. Merutka, W. Cho, W. Welches, F. J. Kézdy, and R. L. Heinrikson. 1984. A new class of phospholipases A_2 with lysine on place of aspartate 49. Functional consequences for calcium and substrate binding. *J. Biol. Chem*. 259:13839–13843.

Marsh, D. 1999. Quantitation of secondary structure in ATR infrared spectroscopy. *Biophys. J*. 77:2630–2637.

Mendelsohn, R. and H. H. Mantsch. 1986. Fourier transform infrared studies of lipid-protein interactions. *In* Progress in Protein-Lipid Interactions. A. Watts and J. J. DePont, editors. Elsevier, Amsterdam. 103–146.

Pan, Y. H., T. M. Epstein, M. K. Jain, and B. J. Bahnson. 2001. Five coplanal anion binding sites on one face of phospholipase A_2: relationship to interface binding. *Biochemistry*. 40:609–617.

Pieterson, W. A., J. C. Vidal, J. J. Volwerk, and G. H. de Haas. 1974. Zymogen-catalyzed hydrolysis of monomeric substrates and the presence of a recognition site for lipid-water interfaces in phospholipase A_2. *Biochemistry*. 13:1455–1460.

Renetseder, R., B. W. Dijkstra, K. Huizinga, K. H. Kalk, and J. Drenth. 1988. Crystal structure of bovine pancreatic phospholipase A_2 covalently inhibited by *p*-bromo-phenacyl-bromide. *J. Mol. Biol*. 200:181–188.

Scott, D. L. and P. B. Sigler. 1994a. Structure and catalytic mechanism of secretory phospholipase A_2. *Adv. Protein Chem*. 45:53–88.

Scott, D. L. and P. B. Sigler. 1994b. The structural and functional roles of calcium ion in secretory phospholipase A_2. *Adv. Inorg. Biochem*. 10:139–155.

Scott, D. L., S. P. White, Z. Otwinowski, W. Yuan, M. H. Gelb, and P. B. Sigler. 1990. Interfacial catalysis: the mechanism of phospholipase A_2. *Science*. 250:1541–1546.

Seelig, J., S. Nebel, P. Ganz, and C. Bruns. 1993. Electrostatic and nonpolar peptide-membrane interactions. Lipid binding and functional properties of somatostatin analogues of charge $z = +1$ to $z = +3$. *Biochemistry*. 32:9714–9721.

Sekar, K., R. Biswas, Y. Li, M.-D. Tsai, and M. Sundaralingam. 1999. Structures of the catalytic site mutants D99A and H48Q and the calcium-loop mutant D49E of phospholipase A_2. *Acta Crystallogr*. D55:443–447.

Six, D. A. and E. A. Dennis. 2000. The expanding superfamily of phosphplipase A_2 enzymes: classification and characterization. *Biochim. Biophys. Acta*. 1488:1–19.

Tatulian, S. A. 1995. Evaluation of divalent cation binding to phosphatidylserine membranes by an analysis of concentration dependence of surface potential. *J. Colloid Interface Sci*. 175:131–137.

Tatulian, S. A. 2001. Toward understanding interfacial activation of secretory phospholipase A_2 (PLA_2): membrane surface properties and membrane-induced structural changes in the enzyme contribute synergistically to PLA_2 activation. *Biophys. J*. 80:789–800.

Tatulian, S. A. 2002. Quantitative characterization of membrane binding of peripheral proteins by spin-label EPR spectroscopy. *J. Phys. Chem*. 106:8870–8877.

Tatulian, S. A., R. L. Biltonen, and L. K. Tamm. 1997. Structural changes in a secretory phospholipase A_2 induced by membrane binding: a clue to interfacial activation? *J. Mol. Biol*. 268:809–815.

Tatulian, S. A., D. M. Cortes, and E. Perozo. 1998a. Structural dynamics of the *Streptomyces lividans* K^+ channel (SKC1): secondary structure characterization from FTIR spectroscopy. *FEBS Lett*. 423:205–212.

Tatulian, S. A., J. Steczko, and W. Minor. 1998b. Uncovering a calcium-regulated membrane binding mechanism for soybean lipoxygenase-1. *Biochemistry*. 37:15481–15490.

Touqui, L. and M. Alaoui-El-Azher. 2001. Mammalian secreted phospholipases A_2 and their pathophysiological significance in inflammatory diseases. *Curr. Mol. Med*. 1:739–754.

Valentin, E., F. Ghomashchi, M. H. Gelb, M. Lazdunski, and G. Lambeau. 1999. On the diversity of secreted phospholipases A_2. Cloning, tissue distribution, and functional expression of two novel mouse group II enzymes. *J. Biol. Chem*. 274:31195–31202.

Verger, R. and G. H. de Haas. 1976. Interfacial enzyme kinetics of lipolysis. *Annu. Rev. Biophys. Bioeng*. 5:77–117.

Verheij, H. M., J. J. Volwerk, E. H. Jansen, W. C. Puyk, B. W. Dijkstra, J. Drenth, and G. H. de Haas. 1980. Methylation of histidine-48 in pancreatic phospholipase A_2. Role of histidine and calcium ion in the catalytic mechanism. *Biochemistry*. 19:743–750.

Volwerk, J. J., W. A. Pieterson, and G. H. de Haas. 1974. Histidine at the active site of phospholipase A_2. *Biochemistry*. 13:1446–1454.

Yang, C. C. and K. King. 1980. Chemical modification of the histidine residue in basic phospholipase A_2 from the venom of *Naja nigricollis*. *Biochim. Biophys. Acta*. 614:373–388.

Yu, B.-Z., M. J. Poi, U. A. Ramagopal, R. Jain, S. Ramakumar, O. G. Berg, M.-D. Tsai, K. Sekar, and M. K. Jain. 2000. Structural basis of the anionic interface preference and k_{cat}* activation of pancreatic phospholipase A_2. *Biochemistry*. 39:12312–12323.

Yu, B.-Z., J. Rogers, G. R. Nicol, K. H. Theopold, K. Seshadri, S. Vishweshwara, and M. K. Jain. 1998. Catalytic significance of the specificity of divalent cations as K_s* and k_{cat}* cofactors for secreted phospholipase A_2. *Biochemistry*. 37:12576–12587.

Yu, B.-Z., J. Rogers, M.-D. Tsai, C. Pidgeon, and M. K. Jain. 1999. Contribution of residues of pancreatic phospholipase A_2 to interfacial binding, catalysis, and activation. *Biochemistry*. 38:4875–4884.

Yuan, C., I. L. Byeon, M.-J. Poi, and M. D. Tsai. 1999. Structural analysis of phospholipase A_2 from functional perspective. 2. Characterization of a molten globule-like state induced by site-specific mutagenesis. *Biochemistry*. 38:2919–2929.

Zhao, H., L. Tang, X. Wang, Y. Zhou, and Z. Lin. 1998. Structure of a snake venom phospholipase A_2 modified by *p*-bromophenacyl-bromide. *Toxicon*. 36:875–886.

Zhou, N. E., C. M. Kay, and R. S. Hodges. 1992. Synthetic model proteins. Positional effects of interchain hydrophobic interactions on stability of two-stranded α-helical coiled-coils. *J. Biol. Chem*. 267:2664–2670.